ELSEVIER

Polymer 42 (2001) 3161–3170

polymer

www.elsevier.nl/locate/polymer

Improved compatibilization in ternary poly(ether imide)/polyarylate–rodrun blends by means of interchange reactions

S. Bastida, J.I. Eguiazabal*, J. Nazabal

Departamento de Ciencia y Tecnología de Polímeros and Instituto de Materiales Poliméricos POLYMAT, Facultad de Química, UPV/EHU Universidad Del Pais Vasco, P.O. Box 1072, 20080 San Sebastian, Spain

Received 7 March 2000; accepted 11 August 2000

Abstract

A possible compatibilization method in thermoplastic/liquid crystalline polymer blends based on the development of interchange reactions between the components of the blends has been tested in the case of the blends of Rodrun (Ro) with a miscible 80/20 poly(ether imide) (PEI)/polyarylate (PAr) thermoplastic matrix. The interchange reactions between PAr and Ro modified the nature of the PAr miscibilized in PEI, improving the adhesion between the modified matrix and Ro as seen by the improved ductility of the blends with 20% Ro. This indicated an additional compatibilization of the blend. The additional compatibilization was not able to overcome the brittle nature of the Ro at large Ro contents (40%), but in the case of the 20% Ro blends, led to blends with overall improved mechanical properties compared to those of the reference blends without additional time in the melt state.

Keywords: Compatibilization; Polymer blends; Interchange reactions

1. Introduction

Blends of thermoplastics reinforced with thermotropic liquid-crystal polymers (TLCPs) are the subject of much current research activity [1–4]. This is mainly due to the potential for the development of new, fully organic, reinforced materials provided by these blends. The reinforcement of the thermoplastic matrix is obtained by the highly oriented fibrillar structures of the TLCP in the solid state. These structures are a consequence of the ordered structure in the melt, which may be attained by means of the shear and elongational flow fields during extrusion or injection moulding. The high stiffness and strength of these fibrillar structures make them very effective reinforcements.

One of the most evident limitations of TLCP-reinforced thermoplastics is the usual total immiscibility of thermoplastics and TLCPs. This gives rise to a high interfacial tension that impedes the dispersion and fibrillation of TLCP, and that gives rise to, when fibrillated, unstable melt structures. Moreover, immiscibility also gives rise to a low interfacial adhesion, which reduces the stress transmission ability of the interphase in the solid state. Both effects lead to mechanical properties of the blends well below the maximum that could be expected from the reinforcing ability of TLCPs. As a consequence, compatibilization methods to reduce the interfacial tension and to improve adhesion are widely sought.

Different compatibilization methods have been used in thermoplastic/TLCP blends. For example, in the widely studied polypropylene (PP) blends [5–11], the modifications by either maleic anhydride-grafted PP [5–7], or ethylene- or propylene-acrylate copolymers [8,9] are the most common. In poly(ethylene terephthalate) (PET) [12], polycarbonate [13,14] and poly(ether imide) [15,16] blends with TLCPs, the incorporation of copolymers able to interact with, or even miscible with the basic blend components, is the most used compatibilization method. Other compatibilizers include ionomers [17,18], and epoxy couplers [19,20].

In a previous work [21], we reported a different compatibilization method in thermoplastic/TLCP blends based on the addition of a second thermoplastic miscible with the matrix and which could interact with the TLCP. The compatibilization was demonstrated in the case of blends of poly(ether imide) (PEI)/Rodrun LC-5000 (Ro), through the addition to the PEI of 20% of a polyarylate (PAr). The compatibilization was attained thanks to the miscibility between PEI and PAr at that composition, and to the interactions between the PAr and Ro, which are a consequence of the polyester nature of both polymers. Both effects decrease the interfacial tension observed through the improved dispersion and fibrillation of the TLCP. The

* Corresponding author. Tel.: +349-43-448000; fax: +349-43-212236.
E-mail address: popegori@sq.ehu.es (J.I. Eguiazabal).

0032-3861/01/$ - see front matter
PII: S0032-3861(00)00630-3

improved morphology and adhesion in the solid state produced mean increases in the Young's modulus and tensile strength of 28 and 75%, respectively, with respect to those of the unmodified PEI/Ro blends.

Furthermore, there is another possible method of improving compatibility. Taking into account that most of the commercial TLCPs are either copolyesters or co-poly(ester-amides), interchange reactions may occur between the blend components in the melt state [22–26] when TLCPs are mixed with condensation thermoplastics such as polyesters or polyamides. These reactions give rise to copolymers of the original blend components [27–29]. These copolymers should improve the compatibility of thermoplastic/TLCP blends. However, this possibility of compatibilization by means of reaction with a third component has not been, to our knowledge, attempted previously in thermoplastic/TLCP blends.

In this paper, a compatibilization method for thermoplastic/TLCP blends, based on the production of a reacted copolymer during the melt processing, will be presented. For this purpose, the PEI/PAr–Ro blends were used because PAr and Ro should react in the melt state owing to their mutual polyester nature. The copolymer produced should improve the compatibility between the matrix and the Ro. For these reasons, the possibility of transesterification reactions between PAr and Ro in the melt state, and their effects on the structure, morphology and mechanical behaviour of the PEI/PAr–Ro blends have been studied. The observed effects are compared with those obtained in the unreacted PEI/PAr–Ro blends. Given that TLCP contents less than 10% did not give rise to reacted products sufficient to produce noticeable improvements in mechanical properties, and that the mechanical properties of the blends did not practically improve [21] with respect to those of the matrix, the study was carried out on blends with TLCP contents of 20 and 40%. The maximum TLCP content was selected taking into consideration the maximum reinforcement content used in short fibre-reinforced thermoplastics. The blends were prepared by a two-stage mixing method in a single-screw extruder and then injection moulded. Additional residence times in the injection moulding machine were used to attain increasing reaction levels. The solid state structure was studied by differential scanning calorimetry (DSC), and the morphology of the blends was analyzed by scanning electron microscopy (SEM). The mechanical properties were determined by means of tensile and impact tests.

2. Experimental

The PEI (Ultem 1000, General Electric), was supplied by Polymerland Guzman (Valencia, Spain) with molecular weights $M_w = 30,000$ and $M_n = 12,000$. The TLCP was a *p*-hydroxy benzoate/ethylene terephthalate (80/20) copolyester commercialized by Unitika Ltd under the trade name Rodrun LC-5000 (Ro). It has an intrinsic viscosity of 0.552 dl/g, as determined at 30°C in a phenol/tetrachloroethane (50/50) mixture. The polyarylate (PAr) was a copolyester of bisphenol-A and a 50/50 mixture of isophthalic and terephthalic acids. It was supplied by Unitika Ltd under the trade name U-Polymer. The average molecular weights of PAr are $M_w = 51,500$ and $M_n = 21,500$, determined by GPC in THF at 30°C.

PEI and Ro were dried before processing for 8 h at 135°C, and PAr for 24 h at 80°C. To prepare the blends, PEI and PAr were first mixed at an 80/20 composition at 330°C using a single-screw extruder (Brabender) driven by a Brabender PLE-650 plasticorder, through a six-element Kenics static mixer. The screw had a diameter of 19 mm, *L/D* of 25 and compression ratio of 2/1. The obtained rod extrudate was pelletized at the exit of the die. In the second stage, dry mixtures of pellets of the PEI/PAr (80/20) and Ro were fed into the extruder to obtain the ternary blends, using the same processing conditions, and the blends were pelletized. The ternary blends will be named as PEI/PAr–Ro (80/20–XX), where XX is the Ro content with respect to the whole blend.

The extruded ternary blends were injection moulded using a Battenfeld BA230E reciprocating screw injection moulding machine. The screw had a diameter of 18 mm and *L/D* ratio of 17.8. The mould provided tensile specimens according to ASTM D-638, type IV, and impact specimens according to ASTM D-256. The injection speed was 23 cm^3/s and the injection pressure, 2850 bar. The melt and mould temperatures were 330 and 85°C respectively. PEI and Ro were also moulded under the same conditions as reference materials. The dwell time between consecutive moulding cycles was the parameter used to obtain additional residence times (a-rt) in the injection machine. The a-rt were obtained by multiplying the duration of a moulding cycle (22 s plus the additional dwell time (s)) by the number of cycles (roughly 5) that the material remained in the injection machine. The minimum dwell time of 2 s corresponded to the shortest reaction time and to a residence time of 2 min in the injection machine. This blend studied in a previous work [21] corresponds to an a-rt = 0 and will be considered as a reference.

The development of interchange reactions between PAr and Ro was studied in a Brabender batch mixer at 330°C and at a 50/50 composition. A rotation rate of 6 rpm was used until a homogeneous blend was obtained. The rotation rate was then increased to 30 rpm, and the blend subjected to additional increasing kneading times, up to a maximum of 12 min.

The phase structure of the blends and the development of interchange reactions were analyzed by DSC using a Perkin–Elmer DSC-7 calorimeter. A first scan was carried out from 30 to 330°C at 20°C/min in order to remove the previous thermal history. After cooling at the maximum speed provided by the calorimeter (approximately 100°C/min), a second scan was carried out under the same experimental conditions. The glass transition temperatures of the

Table 1
Thermal transitions of PAr/Rodrun (50/50) blends as a function of the additional kneading time at 330°C and 30 rpm

Additional kneading time (min)	T_g (PAr, °C)	T_g (Rodrun, °C)	T_m (Rodrun, °C)
0	185	63	279
1	179	63	281
2	170	64	285
4	164	62	286
8	157	66	296
12	155	–	303

blends (T_g), as well as the melting temperature (T_m) of Ro were determined in the usual way. The melting heat was not determined because it was very small (3.6 J/g for the neat Ro) [30] and the melting endotherms were comparatively broad, thus making the measurement difficult. The calorimeter was calibrated with respect to an indium standard, and a nitrogen flow was maintained through the sample and reference chambers. The interchange reactions were also followed by Fourier transform infrared spectroscopy (FTIR) using a Nicolet Magna-IR 560 spectrophotometer.

The morphology of the tensile-broken specimens was studied by scanning electron microscopy (SEM), after gold coating. A Hitachi S-2700 microscope was used at an accelerating voltage of 15 kV.

Tensile tests were carried out in an Instron 4301 tensile tester at room temperature. The mechanical properties (Young's modulus, tensile strength, and ductility, measured as the break strain) were determined from the load-elongation curves. The unnotched Izod impact tests were carried out at room temperature using a Ceast 6548/000 pendulum. At least eight specimens were tested for each reported value in both the tensile and impact tests.

3. Results and discussion

3.1. Transesterification reactions between the PAr and the Rodrun

Both PAr and Ro are polyesters. Therefore [31,32], transesterification reactions may take place between both polymers in the melt state. Such reactions have been seen [33] in PAr blends with a TLCP consisting of the same components as Ro, but in a different proportion. The likely development of transesterification reactions in the blends of PAr with the Ro of this work, would modify the chemical nature of the blends and very probably their melt and solid state characteristics. Therefore, the possible occurrence of reactions was studied by calorimetric analysis (DSC) on a PAr/Ro (50/50) blend (relative composition used in the 80/20–20 blend), subjected to kneading times at 330°C longer than those needed for homogeneous blending. The results are shown in Table 1, where the thermal transitions of the blends versus the kneading time are reported. As can be seen, the physical blend (additional kneading time: 0 min) shows two glass transitions (T_g). The upper T_g is practically identical to that of pure PAr, and the lower one corresponds to that attributed [30] to the ethylene terephthalate units of Ro. Despite the partial miscibility previously found [22,33] between PAr and the copolymer of the same components as those comprising Ro, this T_g behaviour indicates that PAr and Ro are immiscible. The melting temperature of Ro in the blends was practically identical to that of pure Ro, also indicating the immiscibility of the blend.

As can also be seen in Table 1, at increasing kneading times, the upper T_g decreased progressively, indicating the occurrence of reactions. The low-temperature T_g barely changed. However, as in a similar system [33], its intensity decreased with the kneading time, disappearing after an additional blending time of 12 min. This behaviour indicates the increasing development of transesterification reactions, and is probably due to the disappearance of ethylene terephthalate units of the Ro, which are progressively incorporated in the PAr chains. The opposite reaction, i. e. the incorporation of PAr units in the Ro chains, seems to be less important, or at least it gives rise to a much smaller change in the T_g of the Ro phase. These facts agree with the results of a study on interchange reactions in PAr/PET blends [34], where the change in the T_g of PET (whose repeat unit is present in the Ro) was much smaller than that of PAr at reaction times similar to those of the present work.

As can also be seen in Table 1, the T_m of Ro in the physical blend unexpectedly increased 24°C after an additional kneading time of 12 min. This is in contrast with the usual effects of interchange reactions on blends with a crystalline polymer, because the T_m tends to decrease due to the decrease in the length of crystallizable sequences as the reacted copolymers are generated. The behaviour of PAr/Ro blends may be attributed to the fact that as reactions take place and the ethylene terephthalate units disappear from the Ro chains, the length of *p*-hydroxy benzoate segments increases, giving rise to more perfect crystals.

The development of interchange reactions between PAr and Ro was also analyzed by FTIR. Fig. 1 shows the FTIR spectra in the carbonyl region of PAr, Ro and the chloroform-soluble fraction of the PAr/Ro (50/50) blend after an additional kneading time of 12 min. If no reaction took place, the carbonyl absorption band of the soluble fraction of the blend should be coincident with that of PAr. However, as can be seen in Fig. 1, it appears slightly displaced towards that of Ro, and even shows a slight slope change at wavenumbers (1715–1725 cm^{-1}) similar to that of the maximum of the absorption band of Ro. This proves the existence of reactions.

3.2. Solid state behaviour of the reacted ternary blends

In Table 2, the thermal transitions of the reference ternary blend and those of some blends after different a-rt are

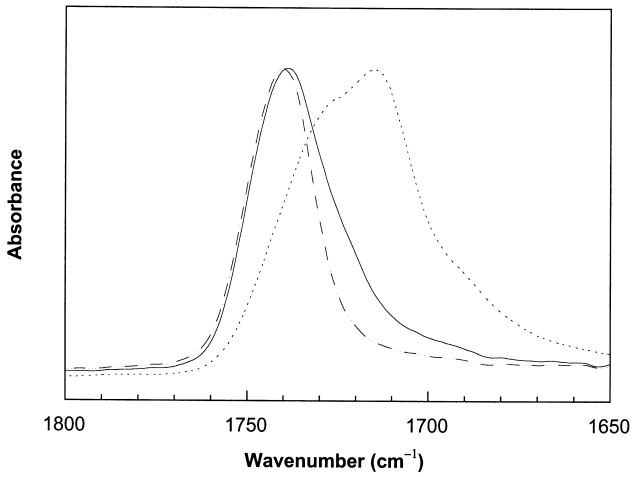

Fig. 1. FTIR spectra in the carbonyl absorption region of PAr (- - -), Ro (·····) and the chloroform-soluble fraction of the PAr/Ro (50/50) blend after an additional kneading time of 12 min (—).

Table 2
Thermal transitions of PEI/PAr–Rodrun blends

	T_g, matrix (°C)		
Additional residence time (a-rt) (min)	80/20–00	80/20–20	80/20–40
0	205	196	195
4.2	–	192	190
8	–	190	187
10.7	–	192	189

shown. The T_m values are not reported because the melting endotherms were very wide, giving rise to a large uncertainty of the results. As can be seen, the observed single T_g corresponds to the matrix, rich in PEI/PAr, because its value is close to the T_g of the miscible PEI/PAr (80/20) blend (203°C) [35,36].The Ro glass transition was not observed. However, the presence of a second Ro phase is clear

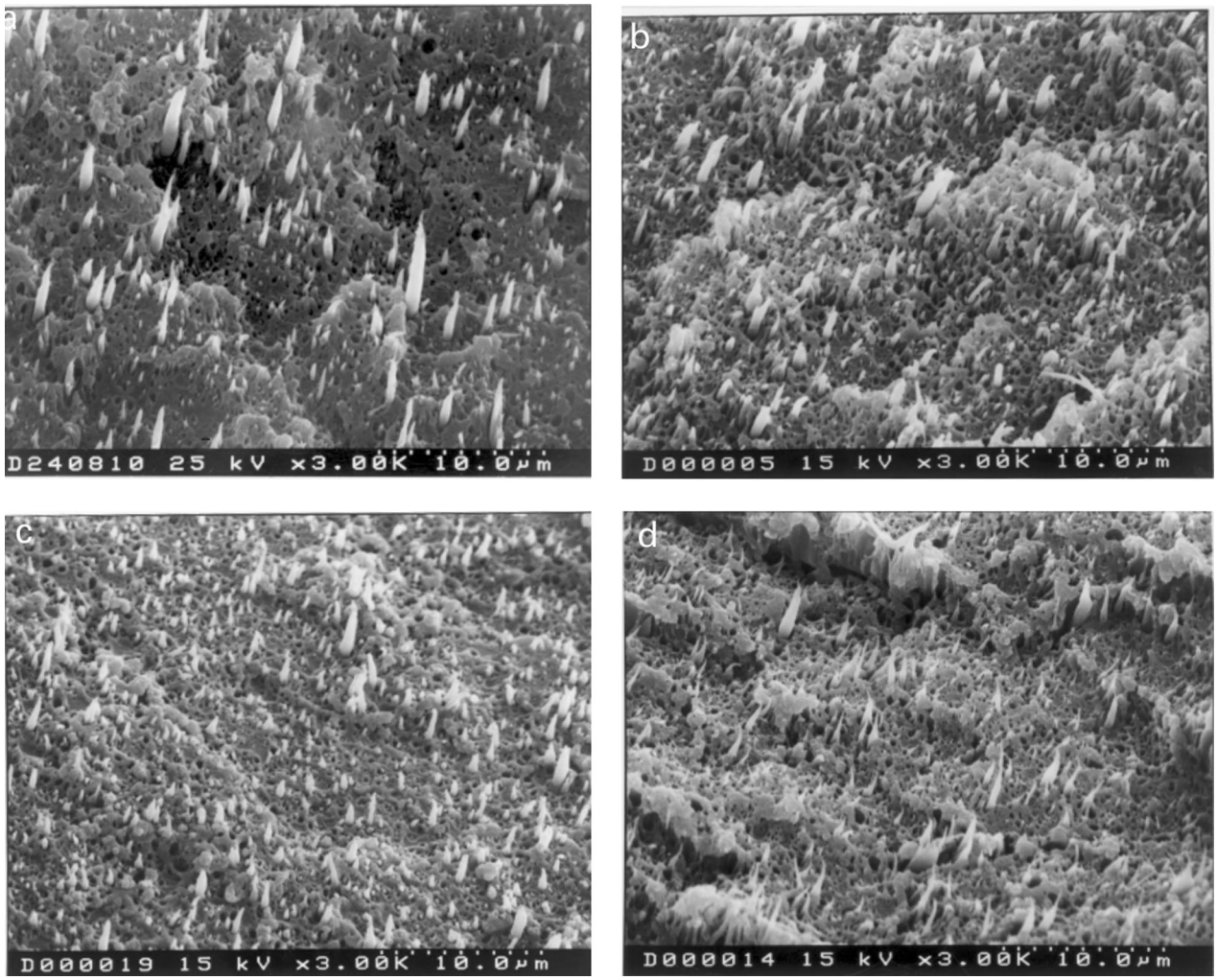

Fig. 2. Tensile fracture surfaces of the skin of the 80/20–20 reference (a) and those of blends obtained with additional reaction time of 1.7 (b), 4.2 (c) and 8 min (d).

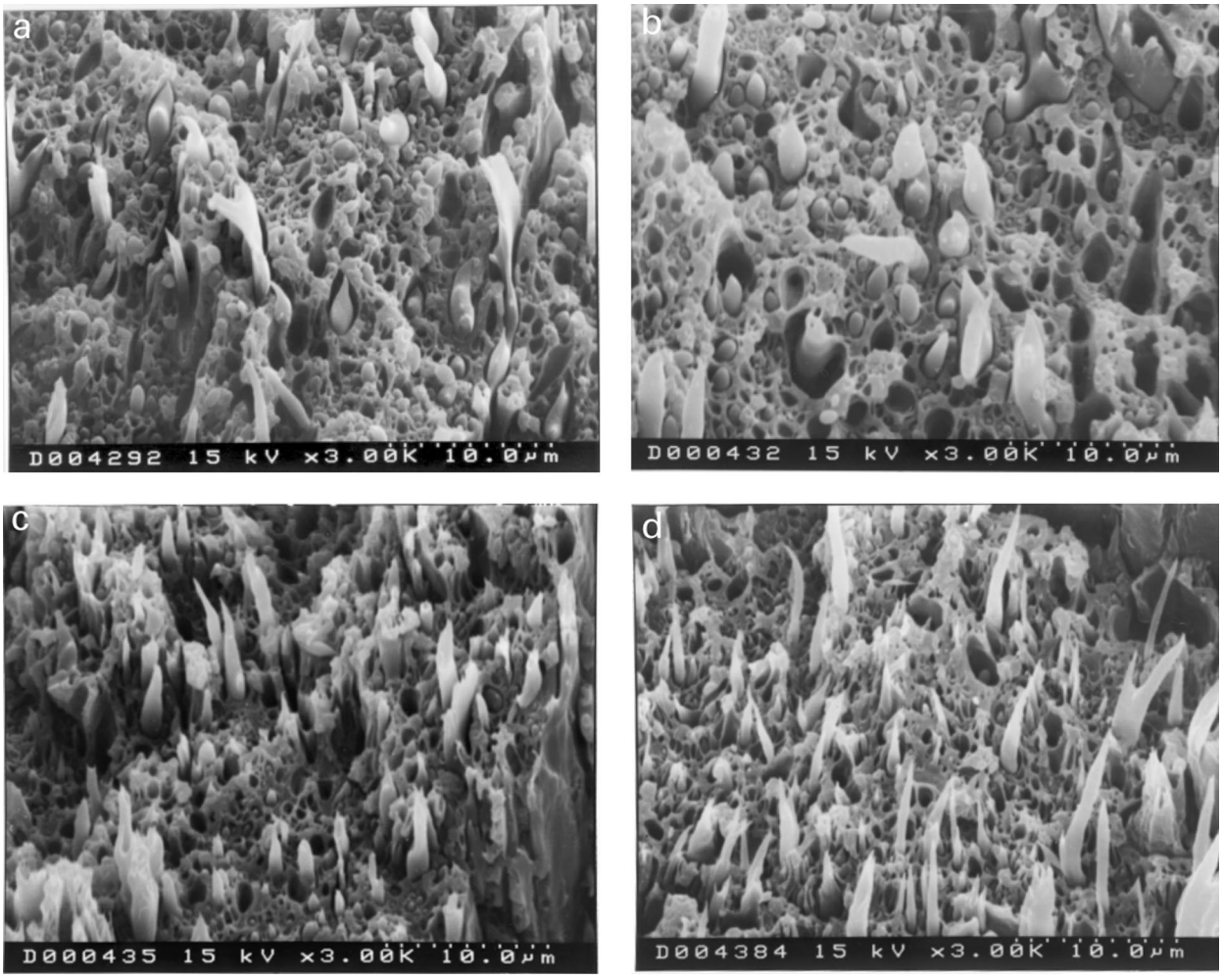

Fig. 3. Tensile fracture surfaces of the skin of the reference 80/20–40 blend (a) and those obtained with additional reaction time of 1.7 (b), 4.2 (c) and 8 min (d).

because the decrease in T_g is too small to be due to the miscibilization of Ro. The non-observance of the T_g of Rodrun was probably due to the small heat capacity change of Ro and to its low content in the blends.

As can be seen in Table 2, in the reference (a-rt = 0) blends, there is a slight (10°C) T_g decrease due to the presence of Ro. It is similar to that previously observed in the binary PEI/Ro blends [37]. This decrease in the T_g induced by the presence of Ro could be attributed to partial miscibility but also, as in PEI/Vectra B950 blends [38], to a more active movement of the TLCP chains in the blends.

As can also be observed in Table 2, the T_g decreased when the residence time increased. The progressive decrease at short times in the T_g of the PEI/PAr matrix clearly indicates the increasing Ro presence induced by the reactions. The effect is less noticeable than that of Table 1, probably due to the smaller possibility of contact between PAr and Ro that the miscibilization of the PAr in the main component PEI offers. As in the 50/50 PAr/Ro blend obtained at the same temperature, discussed in Section 3.1, this behaviour proves that transesterification reactions between both polyesters took place. This is although the impossibility to adequately separate PEI and PAr avoided the study of the interchange reactions in these ternary blends by FTIR. The occurrence of these transesterification reactions and the copolymers that they give rise to, offer an opportunity for their use to improve the compatibility of the blends.

3.3. Morphology

Figs. 2 and 3 show the morphology of the skin of the 80/20–20 and 80/20–40 blends, respectively, after a-rt of 0, 1.7, 4.2 and 8 min. As can be seen in Fig. 2, the dispersed phase particle size decreased after an a-rt of 1.7 min and, although the difference is not so clear, after 4.2 min. In the 80/20–40 blends of Fig. 3, an a-rt between 1.7 and 4.2 min was necessary to thin the dispersed phase. This thinning effect indicates a decrease in the interfacial tension between the matrix and the dispersed phase due to the presence of the reacted copolymers.

In both blends, when the a-rt was 8 min, the size of the Ro particles remained constant or increased slightly. This is not

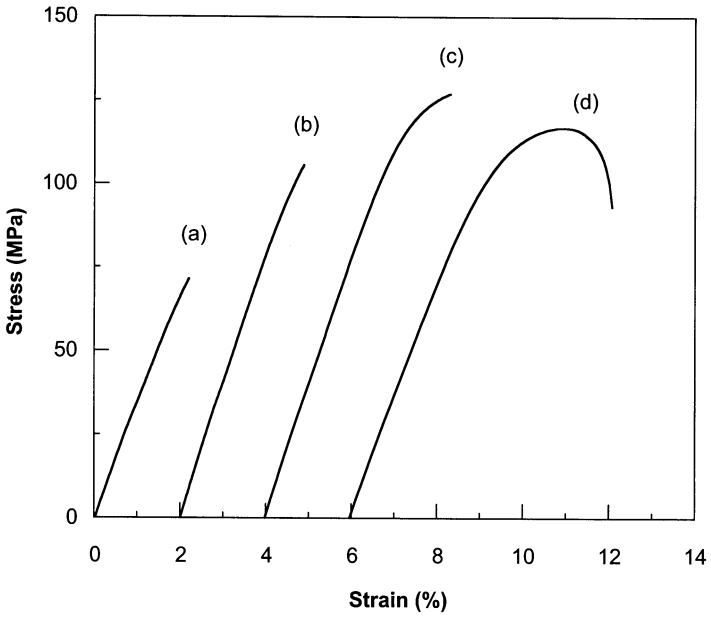

Fig. 4. Tensile curves of the PEI/Ro (80/20) blend (a), of the reference PEI/PAr–Ro (80/20–20) blend (b), and of the reacted PEI/PAr–Ro blend after additional reaction time of 2.5 (c) and 8 min (d).

unexpected because, for example, a slight coarsening was found [16] in PEI/Vectra B950 blends compatibilized with a poly(ester-amide), when the compatibilizer content increased above an optimum value. It was attributed to the flocculation of the TLCP phase as a consequence of strong interparticle interactions. Thus, the presence of reacted copolymers gives rise to an improved Ro dispersion that indicates a decrease in the interfacial tension that probably will lead to an improved adhesion in the solid state.

3.4. Mechanical properties

In Fig. 4, representative tensile curves of the binary 80/20 PEI/Ro blend, of the reference ternary 80/20–20 PEI/PAr–Ro blend, and of two ternary blends after increasing a-rt are shown. As is seen when curves c and d are compared with curve b, they are higher and longer than curve b, which in turn was also higher and longer than that of the binary PEI/Ro blend. This indicates that the effect of the reactions that

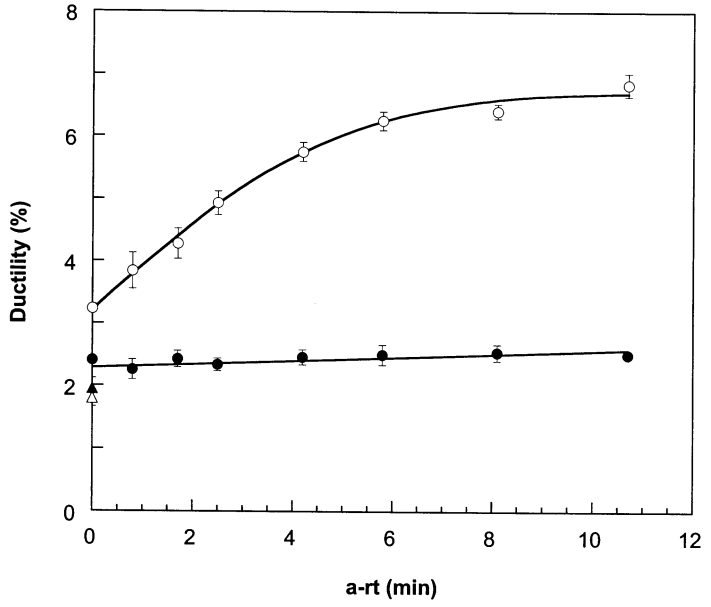

Fig. 5. Ductility of the 80/20–20 (○) and 80/20–40 (●) blends as a function of the additional reaction time. The data for the uncompatibilized 80/20 (△) and 60/40 (▲) blends are represented on the vertical axis.

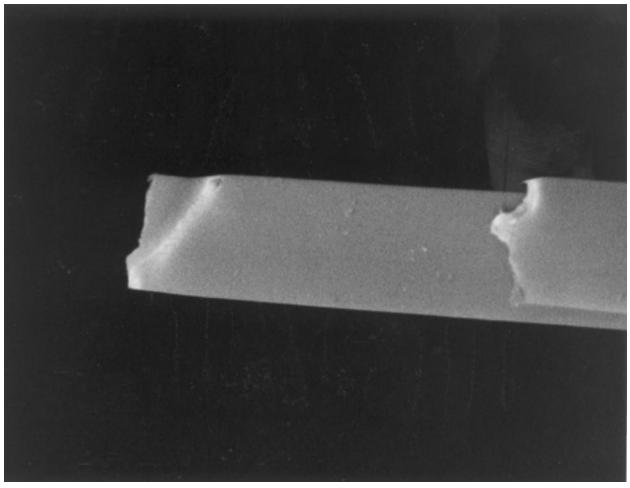

Fig. 6. Fracture region of a 80/20–20 tensile specimen after an additional reaction time of 8 min.

the a-rt gives rise to is to additionally improve the compatibilizing effect of the presence of the PAr compatibilizer.

Fig. 5 shows the ductility of the 80/20–20 and 80/20–40 blends as a function of the a-rt. The ductilities of the binary 80/20 and 60/40 blends are plotted as triangles on the vertical axis. The reference ternary blend, which corresponds to an a-rt = 0, is also plotted on the vertical axis. As can be seen, in the 80/20–40 blends, the ductility did not increase with the a-rt. This was probably due to the important presence of the brittle Ro, which avoided deformations higher than those of its own deformation at break (2.1%) to take place.

As can also be seen, the ductility of the blends with 20% Ro increased with the a-rt up to an a-rt of 6 min. This clearly indicates increasing compatibilization and interfacial adhesion. At longer a-rt, the ductility levelled off, indicating a limiting compatibilization level. The ductility of the blends with 20% LCP is noteworthy because a-rt equal to or greater than 6 min (elongation at break of 6%) gave rise, as can be seen in Fig. 6, to the appearance of shear bands and of partial necking in these blends with 20% TLCP.

Fig. 7 shows the Young's moduli of the blends as a function of the a-rt. The moduli of the binary blends are plotted as triangles on the vertical axis. The values of the reference blends with an a-rt = 0 appear, as in Fig. 5, on the vertical axis. As can be seen, the modulus of the 40% Ro blends first remained constant up to an a-rt of roughly 3 min; it subsequently showed an increase from approximately 5.0 to 5.5 GPa with increasing a-rt. These trends are attributed, respectively, to the observed lack and beginning of production of fibres at roughly the same a-rt. The continuous modulus decrease with a-rt of the 80/20–20 blend was unexpected. The possibility of low adhesion is excluded by the high ductility values of Fig. 5. Thus, the decreasing length of the fibres of Fig. 2 at increasing a-rt may be the reason for the observed behaviour. This is because the short fibres seen in Fig. 2 at a-rt higher than 0 min will probably hinder the effective transmission of stress. Moreover, the modulus decrease was absent at a-rt higher than roughly 7 min, when little change in the fibre length could be observed. Reliable quantitative values for the fibre length could not be obtained due to the complex morphology of the skin and to its indeterminate limit. It might be deduced that the length of the fibres is too short and the decrease in the modulus could indicate that the optimum compatibilization had been reached. However, the observed modulus

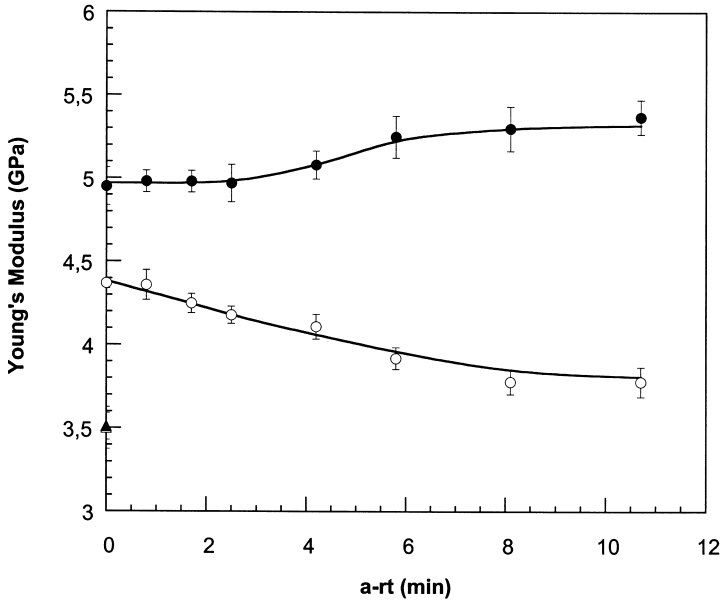

Fig. 7. Young's modulus of the uncompatibilized and compatibilized blends versus the additional reaction time. Symbols as in Fig. 5.

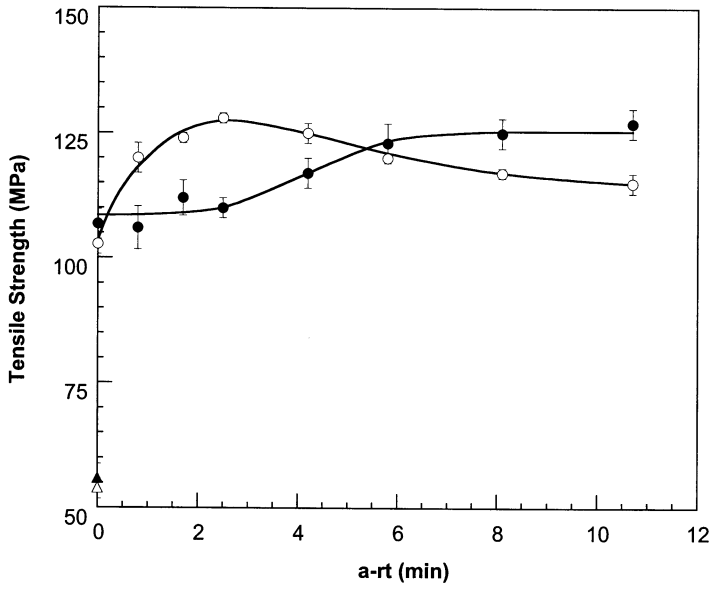

Fig. 8. Tensile strength of the uncompatibilized and compatibilized blends versus the additional reaction time. Symbols as in Fig. 5.

decrease, which was 5–10% in the blends after an a-rt between 2 and 4 min, will be compensated by the higher relative increase in both the tensile and impact strength that the higher ductility permits, as discussed below.

The tensile strengths of the blends as a function of the a-rt are shown in Fig. 8. The shape of the curve of the 40% Ro blends was similar to that of the modulus of elasticity. This is attributed to the fact that another parameter that in these brittle materials controls the tensile strength, i. e. the ductility, remained constant. The maximum increase took place after an a-rt of 5–6 min, and was 16% with respect to that of the reference ternary blend. The initial constancy of the tensile strength coincides with the lack of important change of the morphology that was evident up to an a-rt close to 3 min.

With respect to the tensile strength of the 80/20–20 blend, it increased with the a-rt, attaining at an a-rt of 2–4 min, a maximum value 22% higher than that of the reference PEI/PAr–Ro, and 100% higher with respect to the binary PEI/Ro blend. A qualitatively similar effect was found [16] when an excess of a poly(ester-imide) was added as a compatibilizer in blends of PEI with Vectra B. As can also be seen in Fig. 8, the maximum value in the 40% Ro blends was obtained at a shorter a-rt than in 20% Ro

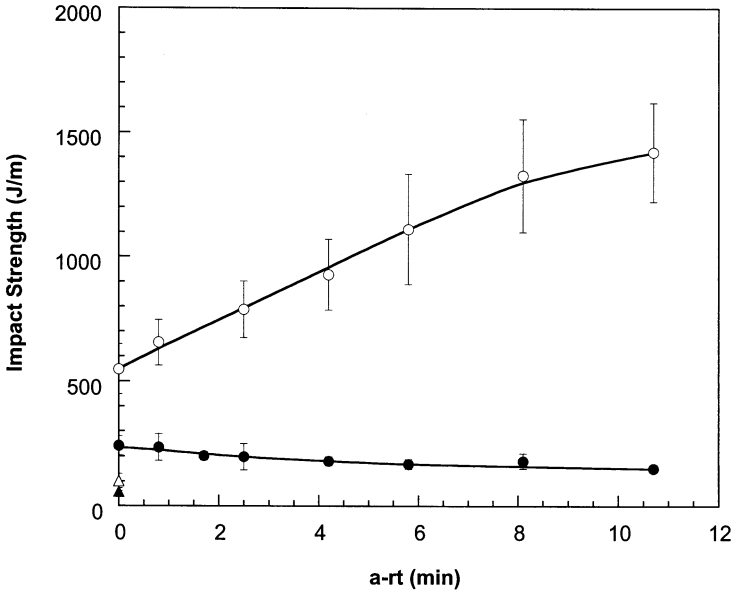

Fig. 9. Unnotched Izod impact strength of the uncompatibilized and compatibilized blends versus the additional reaction time. Symbols as in Fig. 5.

Table 3
Mechanical properties of reinforced PEIs

	Young's modulus (GPa)	Tensile strength (MPa)	Ductility (%)	Unnotched Izod impact strength (J/m)
PEI/PAr–Rodrun (80/20–20)	4.4	131	6.5	1420
PEI/Glass fibre (20 wt%)	6.9	140	3.0	480

blends. This agrees with the fact that the orientation increase was observed faster in the 20% Ro blends than in the 40% Ro blends. The overall behaviour of the tensile strength of the 20% Ro blends is a consequence of the behaviour of the modulus and the ductility. Thus, at an a-rt shorter than roughly 3 min, the negative effect of the decreasing modulus of elasticity is counteracted by the positive effect of the increasing ductility. However, at longer a-rt, where the ductility levels off, the negative effect of the modulus of elasticity is seen.

The unnotched impact strength values are shown in Fig. 9 against the a-rt. The values of the binary blends are plotted on the vertical axis as triangles. The values of the reference blend correspond to an a-rt = 0. As can be seen, the behaviour of the impact strength was rather similar to that of the ductility. As a consequence, the behaviour has to be similar to that of the toughness measured in the tensile test, because the change of the tensile strength was much smaller than that of the ductility. This is due to the low sensitivity of these rather elastic materials to the test speed, and to the unnotched nature of the specimens. As can also be seen, in the case of the 40% Ro blends, the impact strength slightly decreased probably because of the important presence of the brittle Ro. However, the impact strength of the 80/20–20 blend, although clearly smaller than that of the neat PEI (1950 J/m) [35] because of the presence of the brittle Ro, clearly increased with the a-rt. This behaviour is indicative of improved adhesion.

If the mechanical properties of the compatibilized blends are considered as a whole, it appears that for 40% Ro, the increases in the Young's modulus and tensile strength are slight and do not counteract the observed constant ductility and decreasing impact strength. With respect to the 20% Ro blends, the best a-rt is close to 3 min, because the modulus decreases 5% with respect to the reference blend without a-rt, but the increases in tensile strength (15%) and impact strength (25%) are considered to be large enough to positively counterbalance the overall properties. This best a-rt appears to be too long for practical purposes, but it may be easily controlled by means of the addition of catalysts that can be effectively used [31,32] to accelerate interchange reactions.

Finally, the properties of this still unoptimized 80/20–20 blend after an a-rt = 3 min are compared as a reference in Table 3 with those of a commercial PEI also reinforced 20% by weight with short glass fibre (Ultem 2200) [39] (volume percents of 18.6% in Ro and of 11.2% in the case of glass fibre). There is room for a further improvement of the Ro dispersion and fibrillation by optimizing the Ro content, the processing conditions and the compatibilization. However, the balance of properties is not negative. As can be seen, the Young's modulus is clearly higher for the glass fibre-reinforced material (less important if the specific modulus per weight were compared (4.9 GPa/(g/cm^3) against 3.4 GPa/(g/cm^3)). The difference in tensile strength between both reinforced materials is small. The ductility, and probably the toughness in tensile conditions, is 100% higher in the Ro-reinforced PEI. The difference in impact strength is even larger. The smaller abrasive effects on the processing machinery and the ability to flow in the melt state would also improve the competitiveness of TLCP-reinforced composites through increased production and consequent economies of scale.

4. Conclusions

Interchange reactions between PAr and Ro develop in ternary PEI/PAr–Ro blends in the melt state. They give rise to a slight change in the nature of the PAr inside the miscible PEI/PAr matrix. This partially reacted nature of the matrix leads to improved ductility values that indicate an improved interfacial adhesion between the two phases of the blends.

A 40% Ro is too high a content for an effective overall increase in mechanical properties. However, in the case of the 80/20–20 PEI/PAr–Ro blend, additional reaction times (a-rt) of roughly 3 min give rise to a smaller modulus of elasticity owing to the short Ro fibres obtained. This negative effect is counteracted by the higher improvements of the tensile and impact strengths, a consequence of the improved interfacial adhesion and ductility of the blends.

Acknowledgements

The financial support of the Basque Government (Project no. PI96/78) is gratefully acknowledged. S. Bastida also acknowledges the Basque Government for the award of a grant.

References

[1] La Mantia FP. Thermotropic liquid crystal polymer blends. Lancaster: Technomic, 1993.
[2] Acierno D, La Mantia FP. Processing and properties of liquid crystalline polymers and TLCP based blends. Ontario: ChemTec, 1993.
[3] Acierno D, Collyer AA. Rheology and processing of liquid crystal polymers. London: Chapman & Hall, 1996.
[4] Cheremisinoff NP, editor. Handbook of engineering polymeric materials. New York: Marcel Dekker, 1997 (chap. 45).
[5] Heino MT, Seppälä JV. J Appl Polym Sci 1993;48:1677–87.
[6] Datta A, Chen HH, Baird DG. Polymer 1993;34:759–66.
[7] Datta A, Baird DG. Polymer 1995;36:505–14.
[8] Miller MM, Cowie JMG, Tait JG, Brydon DL, Mather RR. Polymer 1995;36:3107–12.
[9] Chiou Y-P, Chiou K-C, Chang F-C. Polymer 1996;18:4099–106.
[10] Holsti-Miettinen RM, Heino MT, Seppälä JV. J Appl Polym Sci 1995;57:573–86.
[11] Yazaki F, Tsubouchi Y, Yosomiya R. Polym Polym Compos 1993;1:183–8.
[12] Poli G, Paci M, Magagnini P, Scaffaro R, La Mantia FP. Polym Engng Sci 1996;36:1244–55.
[13] Singer M, Simon GP, Varley R, Nobile MR. Polym Engng Sci 1996;36:1038–46.
[14] Wei K-H, Ho J-C. J Appl Polym Sci 1997;63:1527–33.
[15] Seo Y, Hong SM, Hwang SS, Park TS, Kim KU. Polymer 1995;36:515–23.
[16] Seo Y, Hong SM, Hwang SS, Park TS, Kim KU. Polymer 1995;36:525–34.
[17] Vallejo J, Eguiazábal JI, Nazábal J. Polymer 2000;41:6311–21.
[18] He J, Liu J. J Appl Polym Sci 1998;67:2141–51.
[19] Chin H-C, Chang F-C. Polymer 1997;38:2947–56.
[20] Chin H-C, Chiou K-C, Chang F-C. J Appl Polym Sci 1996;60:2503–16.
[21] Bastida S, Eguiazábal JI, Nazábal J. Polymer 2001;42:1157–65.
[22] Wang L-H, Porter RS. J Polym Sci Polym Phys Ed 1993;31:1067–73.
[23] Jo B-W, Chang J-H, Jin J-I. Polym Engng Sci 1995;35:1615–20.
[24] Ou C-F, Lin C-C. J Appl Polym Sci 1996;59:1379–87.
[25] Wei K-H, Su K-F. J Appl Polym Sci 1996;59:787–96.
[26] Wei K-H, Ho J-C. Macromolecules 1997;30:1587–93.
[27] Magagnini PL, Paci M, La Mantia FP, Valenza A. Polym Int 1992;28:271–5.
[28] Hong SM, Hwang SS, Seo Y, Chung IJ, Kim KU. Polym Engng Sci 1997;37:646–52.
[29] Lee JY, Jang J, Hong SM, Hwang SS, Seo Y, Kim KU. Int Polym Process 1997;XII:19–25.
[30] Bastida S, Eguiazábal JI, Nazábal J. J Appl Polym Sci 1995;56:1487–94.
[31] Porter RS, Jonza JM, Kimura M, Desper CR, George ER. Polym Engng Sci 1989;29:55–62.
[32] Porter RS, Wang L-H. Polymer 1992;33:2019–30.
[33] Tyan H-L, Wei K-H. J Polym Sci Polym Phys Ed 1998;36:1959–69.
[34] Eguiazábal JI, Ucar G, Cortázar M, Iruin JJ. Polymer 1986;27:2013–8.
[35] Bastida S, Eguiazábal JI, Nazábal J. Eur Polym J 1999;35:1661–9.
[36] Bastida S, Eguiazábal JI, Nazábal J. Polymer 1996;37:2317–22.
[37] Bastida S, Eguiazábal JI, Nazábal J. J Mater Sci 2000;35:153–8.
[38] Lee S, Hong SM, Seo Y, Park TS, Hwang SS, Kim KU, Lee JW. Polymer 1994;35:519–31.
[39] General Electric Plastics. Technical Information on Ultem Resins.